Electronic Supplementary Material (ESI) for Journal of Materials Chemistry A.

Flexible quintuple cation perovskite solar cells with high efficiency

Bingbing Cao,[a] Longkai Yang,[a] Shusen Jiang,[a] Hong Lin,*[b] Ning Wang*[c] and Xin Li*[a]

[a] Pen-Tung Sah Institute of Micro-Nano Science and Technology, Xiamen University, 361005 Xiamen, China. Email: lixin01@xmu.edu.cn

[b] State Key Laboratory of New Ceramics & Fine Processing, School of Material Science and Engineering, Tsinghua University, 100084 Beijing, China. Email: hong-lin@tsinghua.edu.cn

[c] State Key Laboratory of Marine Resource Utilization in South China Sea, Hainan University, 570228 Haikou, China. Email: wangninguestc@gmail.com

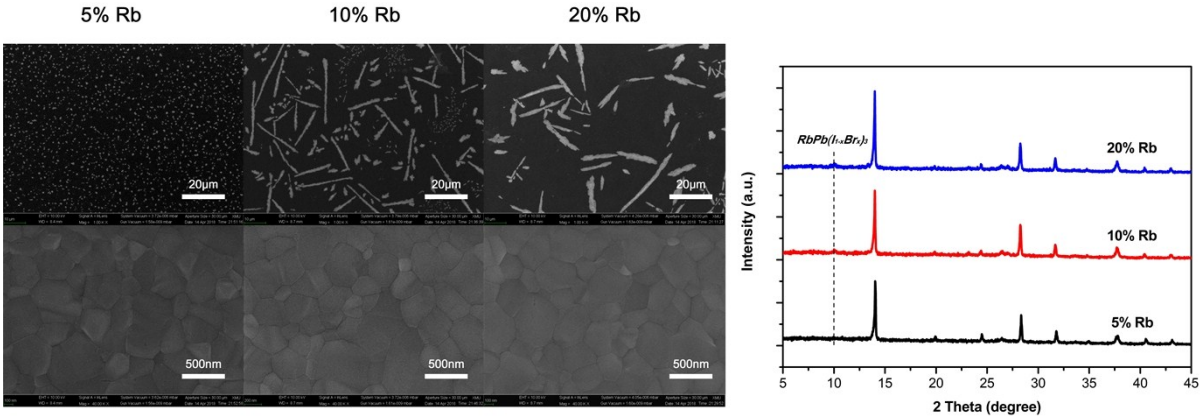

Fig. S1. SEM and XRD of RbCsFAMA films with different Rb^+ cation additions.

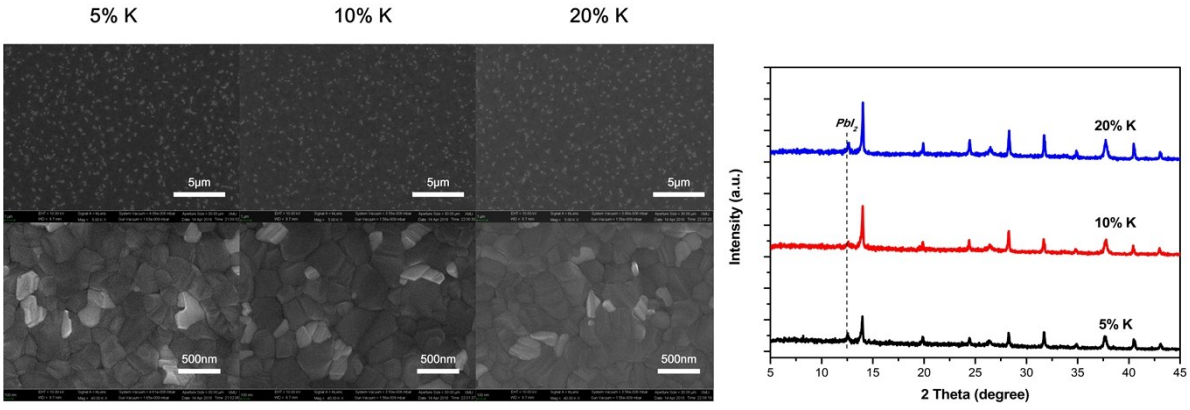

Fig. S2. SEM and XRD of KCsFAMA films with different K^+ cation additions.

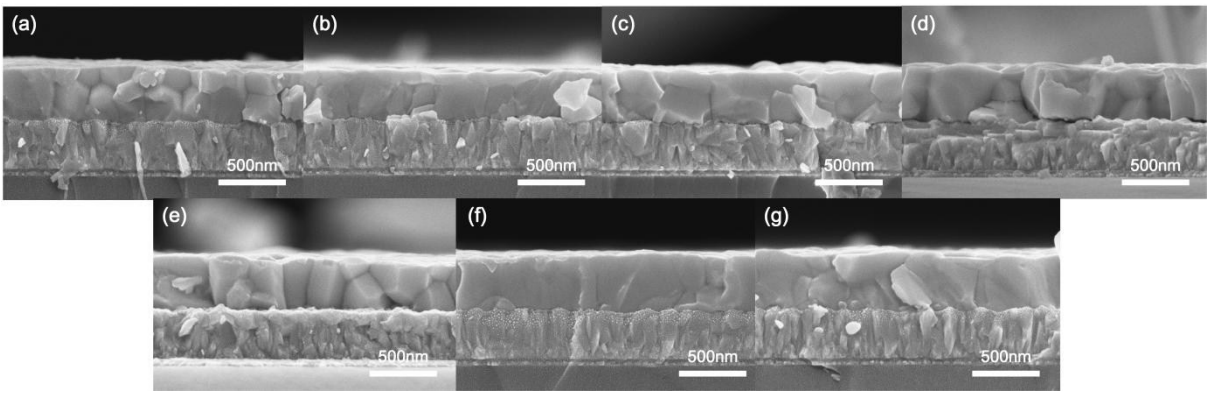

Fig. S3. Cross-section SEM images of different perovskite films: a) CsFAMA (Control), b) $Rb_5CsFAMA$, c-f) $Rb_{5-x}K_xCsFAMA$ (x varies from 1 to 4), and g) $K_5CsFAMA$

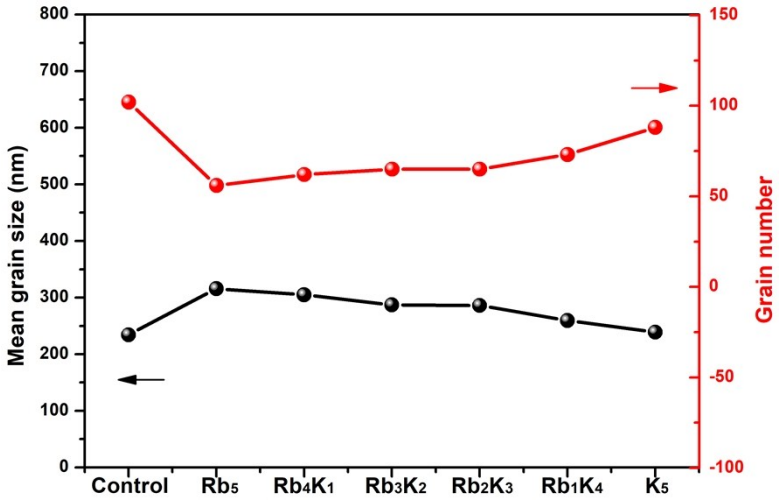

Fig. S4. The mean grain size and grain number of different perovskite films in Fig. 2.

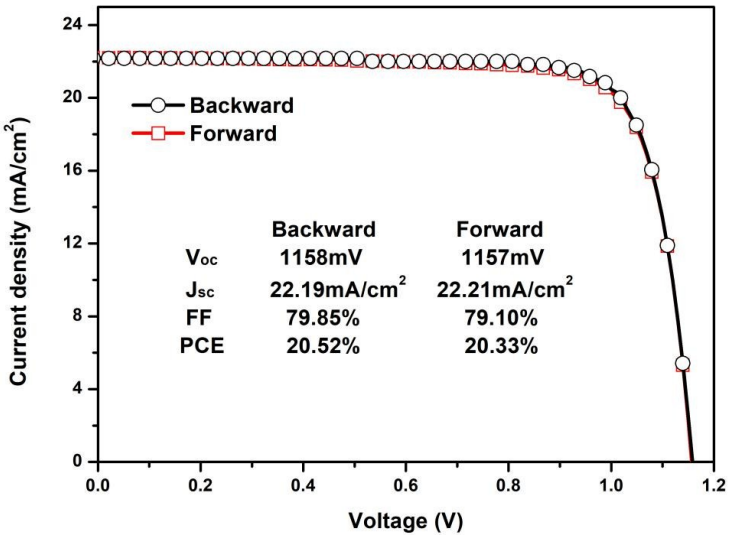

Fig. S5. The J–V curves of the champion device based on $Rb_1K_4CsFAMA$ perovskite measured under backward-scan and forward-scan direction

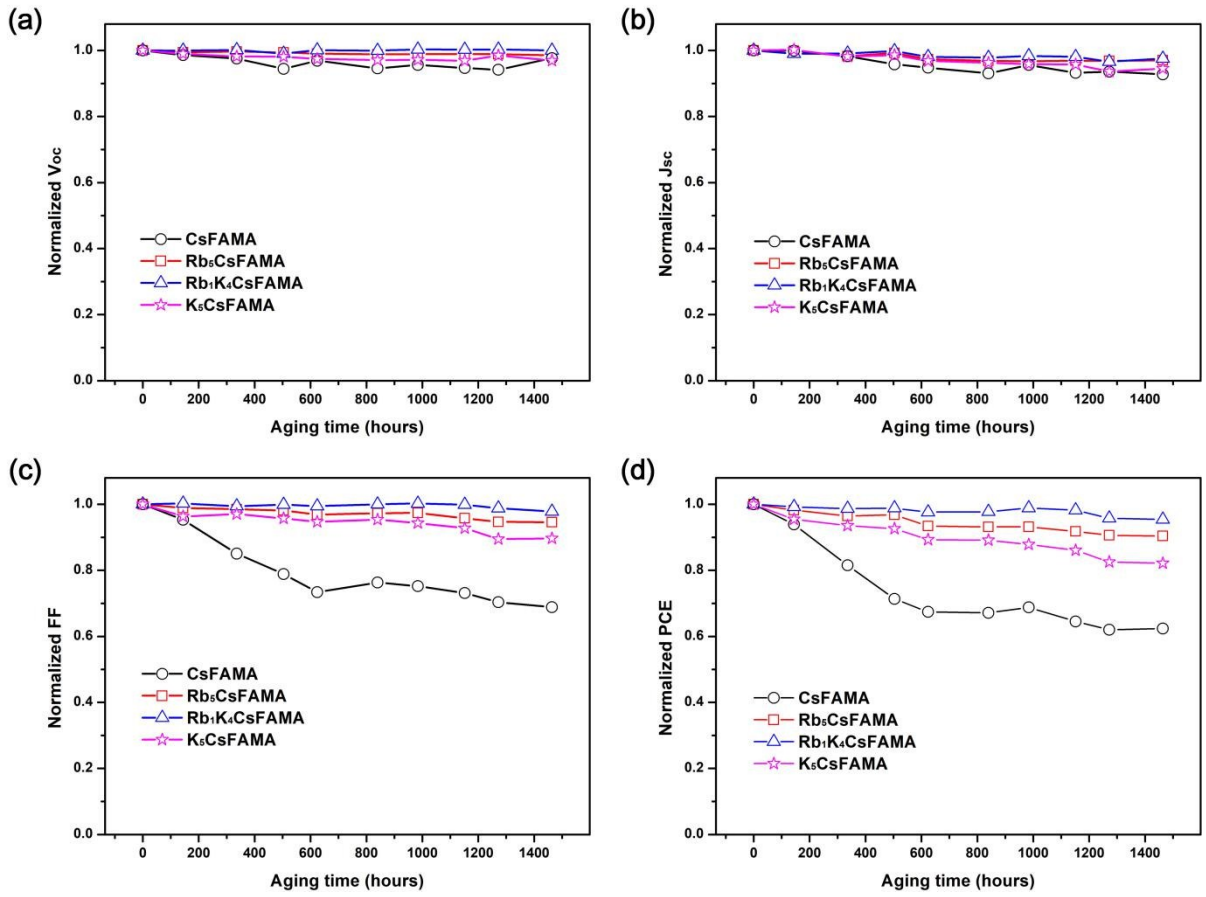

Fig. S6. Long-term stability parameters of devices with different perovskite recipes without encapsulation, under controlled ambient conditions at approximately 10% relative humidity.

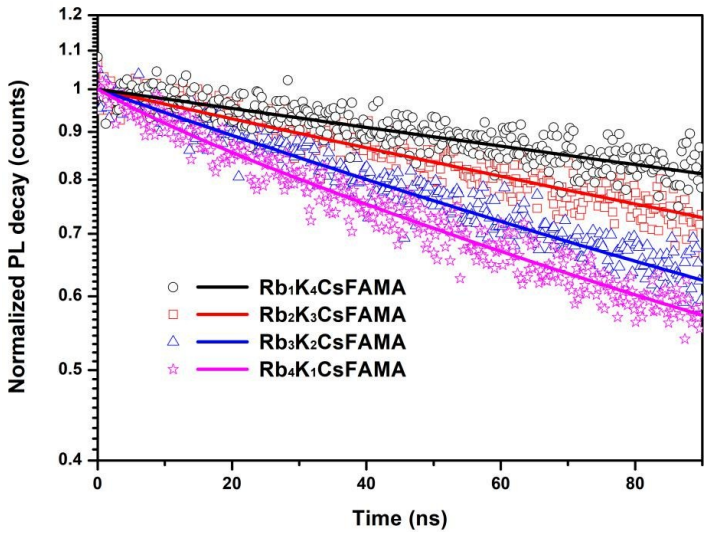

Fig. S7. Time-resolved photoluminescence (TRPL) decay of the perovskites films, $Rb_{5-x}K_xCsFAMA$ (x=1-4) on bare glasses.

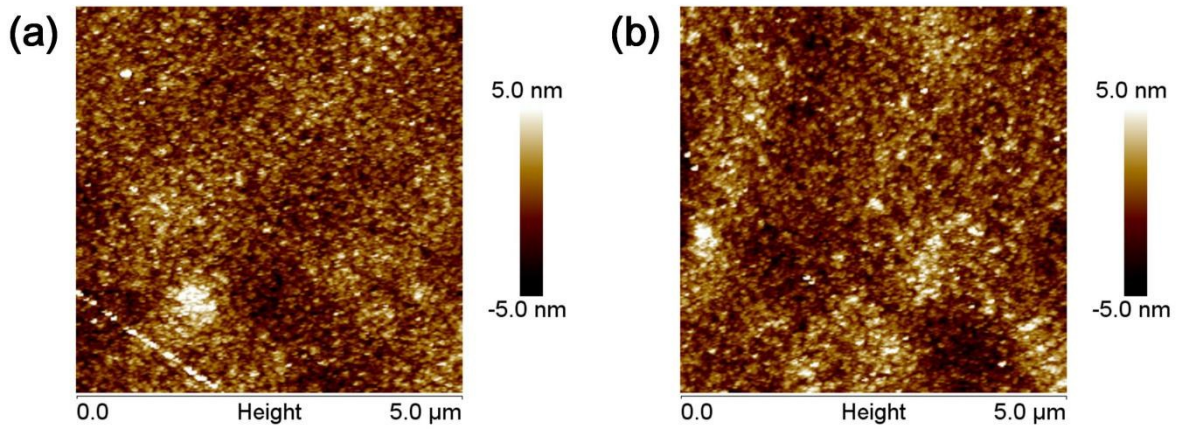

Fig. S8. AFM images of the SnO_2 layers on (a) ITO surface and (b) ITO/HfO_2 surface, respectively.

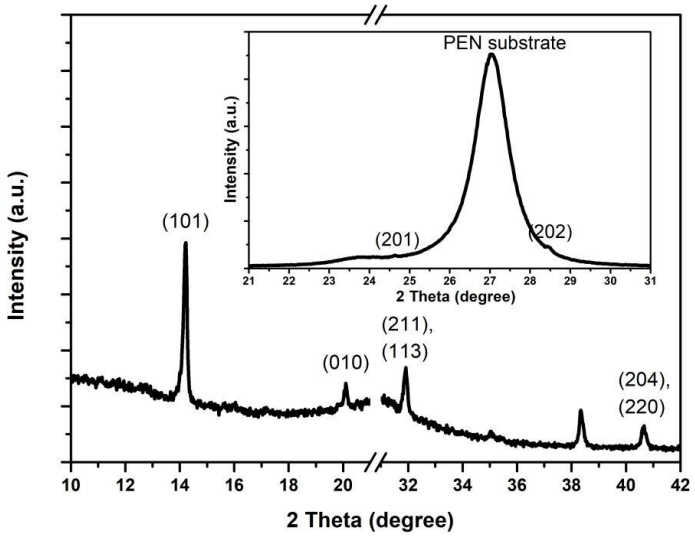

Fig. S9. XRD pattern of the $Rb_1K_4CsFAMA$ perovskite layer on top of ITO/HfO_2/SnO_2.

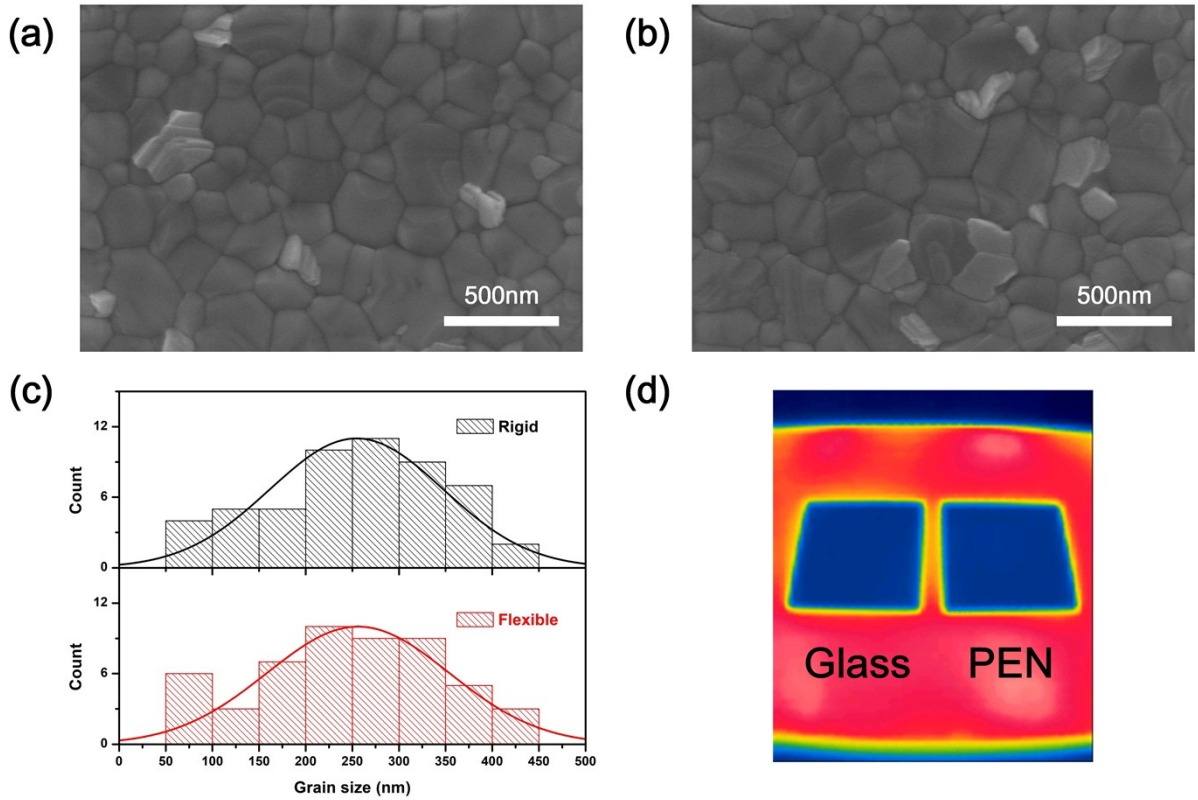

Fig. S10. Surface morphology of (a) the perovskite film on PEN/ITO/HfO_2/SnO_2 and (b) the perovskite film on Glass/FTO/SnO_2. (c) shows the distribution of their grain sizes and (d) shows the infrared thermographs of different substrates using an infrared thermometer (FLIR TG165) (The surface temperatures of the hot plate and the two substrates are 110 ^oC and 61^oC, respectively)

It can be seen from Fig. S10. that the morphology of the perovskite on the flexible substrate and the rigid substrate barely change. Previous study showed that the roughness of the underlayer of perovskite has no effect on the perovskite layer.[1] The heating condition is one of the key factors affecting the perovskite film crystallization.[2] Considering the different thermal properties of flexible substrates and the rigid substrates, we compared the two substrates on hot plate as shown in Fig. S10(d). It can be seen that there is no obvious difference between the two heated substrates. Hence, the perovskite morphologies shown in Fig. S10 (a) and Fig. S10 (b) are almost the same.

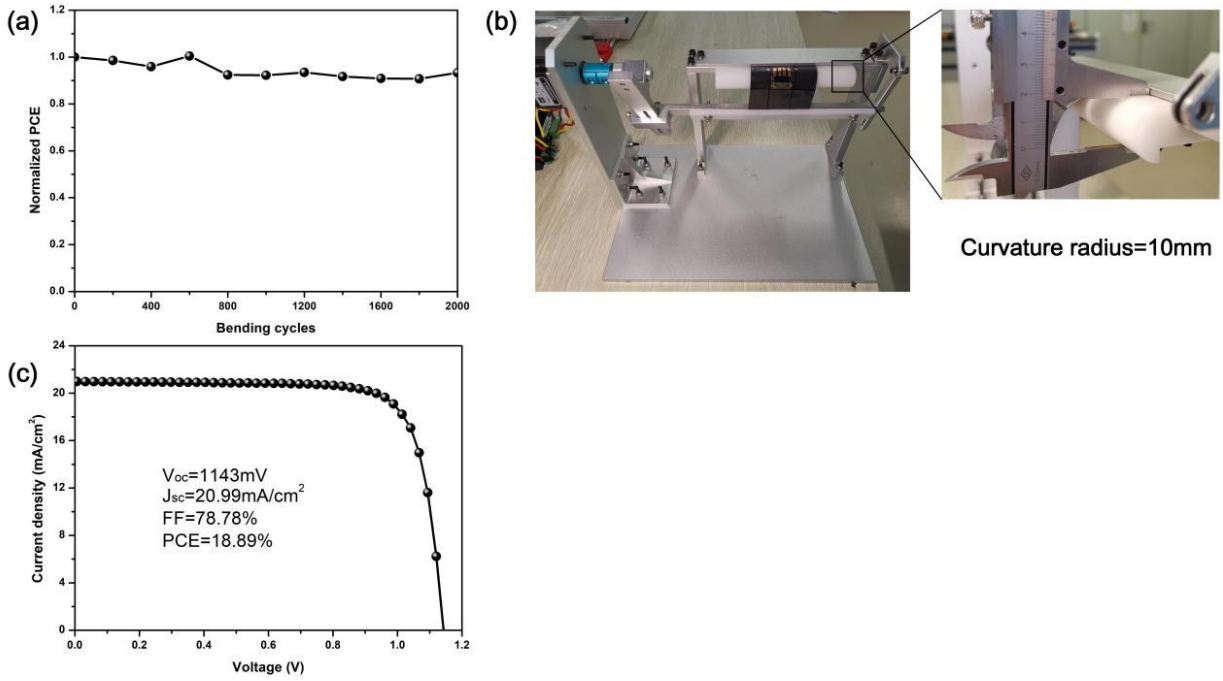

Fig. S11. (a) Normalized PCE of the $Rb_1K_4CsFAMA$-based flexible device as a function of bending cycles with a curvature radius of 10 mm; (b) The graph of our home-made bending machine and (c) The initial IV curve of the tested device.

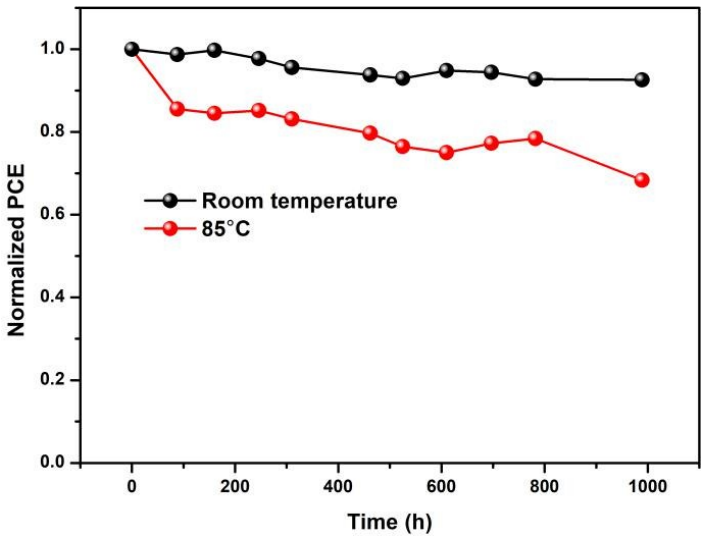

Fig. S12. PCE decay of devices kept at controlled ambient conditions at approximately 10% relative humidity; and kept at 85 in a N_2 environment in dark (To avoid the degration of Spiro-oMeTAD at 85 ° C, 10 wt% of CuPc was added to the hole transport film). Values are the averages for six devices.

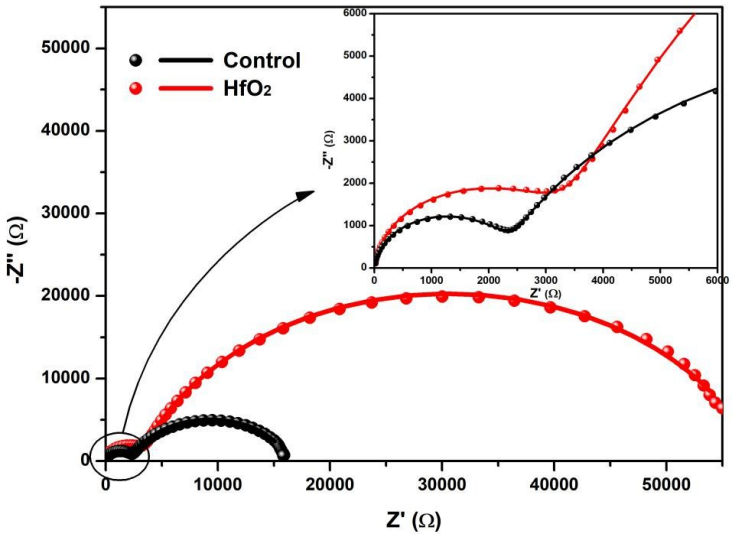

Fig. S13. Nyquist plots of the flexible PSCs with/without HfO_2 layer.

Table S1. The photovoltaic parameters of the rigid PSC devices containing different monovalent cations.

Samples (15 average)	Voc (V)	Jsc (mA cm^{-2})	FF (%)	PCE (%)	Hysteresis index (%)
CsFAMA	1.09±0.01	21.65±0.26	77.38±1.34	18.32±0.49	13.28±3.49
Rb_5CsFAMA	1.11±0.01	21.25±0.28	79.25±1.34	18.68±0.50	11.14±3.15
Rb_4K_1CsFAMA	1.12±0.01	21.51±0.25	79.30±1.38	19.03±0.24	3.62±1.71
Rb_3K_2CsFAMA	1.13±0.01	21.84±0.10	79.07±0.72	19.46±0.24	2.15±0.75
Rb_2K_3CsFAMA	1.13±0.00	21.96±0.17	79.39±0.58	19.75±0.17	1.85±0.79
Rb_1K_4CsFAMA	1.14±0.01	22.20±0.16	79.21±0.30	20.13±0.15	0.89±0.36
K_5CsFAMA	1.12±0.01	21.86±0.16	78.35±0.65	19.15±0.24	3.12±1.23

Table S2. Lifetimes of different perovskites on bare glasses based on photoluminescence decay data. The data were fitted to exponential decay ($y=y_0+A_1\exp[-(x-x_0)/\tau]$).

Samples	τ (ns)
CsFAMA	27.98
Rb_5CsFAMA	38.01
Rb_4K_1CsFAMA	86.52
Rb_3K_2CsFAMA	128.71
Rb_2K_3CsFAMA	215.97
Rb_1K_4CsFAMA	333.25
K_5CsFAMA	180.48

Table S3. The photovoltaic parameters of the flexible PSC devices containing with different HfO_2 layers from different ALD cycles.

Samples (10 average)	Voc (V)	Jsc (mA/cm^2)	FF (%)	PCE (%)
Control	1.11±0.01	20.17±0.08	77.62±0.86	17.43±0.15
2 cycles	1.13±0.01	20.85±0.11	77.66±0.79	18.29±0.15
5 cycles	1.13±0.01	21.07±0.17	78.21±0.72	18.68±0.26
8 cycles	1.10±0.01	20.29±0.13	79.52±1.06	17.80±0.25
11 cycles	1.07±0.01	19.93±0.09	78.84±0.92	16.89±0.31

References

[1] Song, S.; Kang, G.; Pyeon, L.; Lim, C.; Lee, G.; Park, T.; Choi, J., ACS Energy lett., 2017, 2, 2667-2673.

[2] Ye, J.; Zheng, H.; Zhu, L.; Zhang, X.; Jiang, L.; Chen, W.; Liu, G.; Pan, X.; Dai, S.; Sol. Energy Mater. Sol. Cells, 2017, 160, 60-66.